

SHIP-BASED OBSERVATIONS OF CLOUD SURFACE RADIATIVE FORCING DURING THE DYNAMICS OF THE MADDEN-JULIAN

J7.1 OSCILLATION (DYNAMO) FIELD PROGRAM

C.W. Fairall^{1*}, Simon DeSzoeko², J. B. Edson³, Chris Zappa⁴, Alan Brewer¹, Dan Wolfe¹, Ludovic Bariteau¹, Sergio Pezoa¹

1. NOAA, Earth System Research Laboratory, Boulder, Colorado, USA; 2. Oregon State University; 3. University of Connecticut; 4. Columbia University

1. INTRODUCTION

Radiative cloud forcing (CF) – defined as the difference between the observed radiative flux and the flux that would be observed in clear skies – is a simple index of the influence of clouds on the surface heat budget. In this paper we will present measurements of surface CF obtained during the DYNAMO field program aboard the R/V *Revelle*. DYNAMO was conducted in the India Ocean between September 2011 and January 2012. *Revelle* conducted four cruise legs with much of the operations near 0 S 80 E. Solar and IR downward fluxes were observed with a mix of standard thermal radiometers. Our analysis will include linking CRF to simple bulk cloud properties (cloud fraction and integrated liquid water content). We will show that radiative CF dominates the variability of the net heat surface budget. Results from DYNAMO will be compared with several recent tropical convection field programs (TOGA COARE, JASMINE, and EPIC).

2. BACKGROUND ON CLOUD FORCING

Cloud forcing (CF) provides an indication of the impact of clouds on the surface energy budget, and this analysis demonstrates the particular emphasis of our observations in the DYNAMO region.

* Corresponding author address: C. W. Fairall, NOAA ESRL R/PSD03, 325 Broadway, Boulder, CO 80305-333, email: Chris.Fairall@noaa.gov

Cloud forcing is the difference in the observed mean radiative flux versus what the flux would be in the absence of clouds:

$$CF_x = \langle R_x \rangle - \langle R_{x0} \rangle, \quad (1)$$

where R is the radiative flux, the subscript $x = s$ for solar or $x = l$ for longwave (IR), and the subscript 0 refers to the clear-sky flux. Radiative flux sensors provide direct measurement of downward radiation. Estimates of clear-sky flux are computed using so-called clear-sky algorithms which are typically tuned to the regions (we use the algorithms of Fairall et al. 2008).

A related variable that is often used is the *maximum* cloud forcing, which is the conditional change in the flux when a cloud is actually present:

$$MCF_x = \langle R_{x1} \rangle - \langle R_{x0} \rangle \approx \frac{CF_x}{f}, \quad (2)$$

where R_{x1} is the radiative flux for overcast conditions and f is cloud fraction. CF averages clear and cloudy periods, but MCF is the difference between overcast (cloud fraction, $f = 1.0$) and clear ($f = 0$) conditions. MCF is related to the radiative properties of individual clouds and can, in principle, be directly computed from microphysical and radiative variables, while CF is strongly dependent on whether it is cloudy or not. MCF may also be applied in simple models that use cloud fraction to estimate cloud effects on radiative fluxes. In the simplest case, each cloud's radiative properties are similar to all others, and then CF depends upon the number of clouds in the field. Thus, the radiative flux at the surface can be written

$$R_x = R_{x0} + f * MCF_x = (1 - f)R_{x0} + fR_{x1}.$$

(3)

For this paper, we will use the CF of the *net* surface flux (SCF), which is the quantity most relevant to the surface heat balance of the ocean. Net SCF is downward flux multiplied by $1 - \alpha$ (where α is albedo, and is estimated as $\alpha=0.055$ for solar wavelengths over the sea) or multiplied by the broadband IR emissivity (ϵ) of seawater (estimated as 0.97). CF has seen extensive application as an index of the importance of clouds for the global heat balance. This variable yields valuable information about cloud dynamics (Pincus et al. 1997) and is an important tool for diagnosing GCM treatments of cloud/radiative processes. Ramanathan et al. (1995) showed a direct link between surface cloud forcing and oceanic dynamics.

Previous studies in the tropics have shown that the heavy water vapor burden in the boundary layer partially masks the longwave (LW) signal from clouds, and SCF is dominated by the solar flux, as LW SCF is about 5 to 65 Wm^{-2} while shortwave (SW) SCF ranges from -20 to -200 Wm^{-2} . In subtropical stratocumulus regimes, the solar component is more nearly balanced by the LW component and the total SCF is perhaps closer to -30 Wm^{-2} . Thus, SW versus LW compensating effect depends strongly on latitude and season. Tropical regions have the strongest solar cloud forcing, while polar areas tend to have the strongest relative IR cloud forcing. In the upper midlatitude storm track, total SCF tends to be small because the solar and IR components approximately cancel. These relationships can be illustrated with the cloud forcing phase diagram (Cronin et al. 2006; Fairall et al. 2008). When the slope of the line is one, net SFC is zero (i.e., SW cancels LW). An example from the equatorial E. Pacific (Fairall et al. 2008) is shown using daily mean values (Fig. 1). Rather than tending to lie near a single characteristic line, the PACS/EPIC data are scattered from tropical to storm track lines. This indicates that all three principal climate zones (tropical, trade wind, and stratocumulus) are encountered within 10 degrees of the equator in the eastern Pacific.

3. DYNAMO FIELD PROGRAM

DYNAMO was a multi-month field program in the Indian Ocean to investigate convective clouds, the eastward-propagating convective envelope of the Madden Julian Oscillation (MJO), and its coupling to the ocean mixed layer. A team of scientists from NOAA, University of Connecticut, Oregon State University, and Columbia University made a suite of observations from *R/V Revelle* (Fig. 2) in the Indian Ocean during DYNAMO to measure surface air-sea fluxes, MABL turbulent mixing, and cloud and precipitation development. Our strategy is to seamlessly measure processes, from the surface to the MABL and the free troposphere, contributing to tropical convection constituting the MJO. We equipped *Revelle* with radiative sensors and turbulent flux sensors that observe covariances of near-surface temperature, humidity, and velocity; and measure below-cloud mixing and turbulent velocities in the MABL with a scanning Doppler lidar. We also installed a cloud observing system consisting of a lidar ceilometer, a multi-channel microwave radiometer measuring integrated liquid and vapor, and a W-band (3.17 mm) Doppler cloud radar, which provides a sensitive vertical profile of cloud liquid water drops, in-cloud turbulence, and precipitation over the life cycle of the cloud.

Revelle's operations in DYNAMO consisted of four cruise legs principally near 0 deg. latitude and 80 deg. E. longitude between Sept. 1 and Jan. 5 (Fig. 3). For the cloud forcing analysis presented here, our direct observations of surface turbulent heat fluxes, radiative fluxes, cloud fraction, near-surface meteorology, and cloud liquid water will be used. The four cruise legs produced 123 days of data. The net heat flux components are shown in Fig. 4 and the CF in Fig. 5 (data restricted to longitude west of 90 deg. E).

4. DYNAMO CLOUD FORCING ANALYSIS

Daily-average cloud forcing observations from DYNAMO are shown in Fig. 6 on the CF phase diagram. They are quite tightly clustered on the nominal tropical regime line. Fig. 7 shows the data plotted as a function of cloud fraction. The results are similar to the equatorial E. Pacific

(EPIC – Fairall et al. 2008) except the solar cloud forcing is, on average, stronger. However, the EPIC dataset has many observations outside of the deep convection region. Values from the ITCZ are more like the DYNAMO results. The similarity for the IR SFC follows from the strong masking effect of subcloud water vapor that is common in the tropics. Using simple criterion based on cloud fraction, wind speed, and precipitation we have classified the time series for legs 2 and 3 in terms of suppressed (27 days), disturbed (25 days), and MJO regimes (22 days). Fig. 8 shows the SFC as a function for cloud fraction for the regime-averaged data. For example, in typical MJO conditions the cloud fraction is 0.4, the net IR flux is increased by about 25 W/m² while the net solar flux is decreased by 145 W/m². Thus, net radiative SFC during the MJO is -120 W/m² versus -25 W/m² during suppressed conditions.

We also did a simple correlation analysis of SFC against cloud fraction and liquid water path (LWP) from the microwave radiometer. Correlation coefficients with cloud fraction are 0.86 (LW) and -0.70 (SW); correlation with LWP are 0.50 (LW) and -0.27 (SW). The cloud fraction – LWP correlation is only 0.4, which reflects both the distribution of cloud thickness at a given cloud fraction and the somewhat noisy nature of the LWP observation via microwave radiometer.

5. TROPICAL SURFACE ENERGY BALANCE

Radiative SCF tends to dominate the net surface energy budget but radiation is not the only surface flux component affected by convective regimes. To lend context to the DYNAMO results we include an analysis of the mean values of the energy balance over longer time scales (on the order of several weeks) in suppressed vs strongly forced convective regimes. We draw on the existing database of PSD tropical field programs. These are described in Webster et al. (2002) and Fairall et al. (2008). Briefly stated, the field programs are:

TOGA COARE – a 3 month study of MJO and surface fluxes in the equatorial W. Pacific.

JASMINE – a 40-day study of pre-monsoon and monsoon convection in the Bay of Bengal.

EPIC – A multi-year set of 1-month cruises in the equatorial E. Pacific and the ITCZ.

Table I shows the mean surface energy components from these cruises. The means are taken for cruise legs or broken down by convective regimes. In Fig. 9 we show correlations of the sensible, latent, and net-IR fluxes with the net solar flux across this database. The reduction in solar flux can be considered a surrogate for convective disturbance. From Fig. 9 we can see that lower solar flux (increased convective disturbance) is associated with decreased IR cooling (a net warming in the IR) but increased cooling by sensible and latent heat. The sensible and latent heat effects are substantial and reflect the stronger winds and decreased near-surface air temperature under strong convection. A summary graph in terms of net heat flux is shown in Fig. 10. The individual point fall surprisingly close to the nominal line with the only outliers at the extremely suppressed end of the range. Here the net is the same for each region but the solar flux is less in the E. Pacific and greater in the Indian Ocean. The line shown in this figure is

$$H_{net} = -280 + 1.54 * R_{nSolar} \quad (4)$$

6. CONCLUSIONS

The DYNAMO field program yielded a wealth of observations of the atmosphere, ocean, and interface. In this paper we report a brief analysis of one simple aspect – forcing of the surface energy budget by deep convection associated with the MJO and less organized disturbances. The mean net heat balance over the DYNAMO field program is 40 W/m² (net heating that is presumably balanced by advective and entrainment cooling) This balance is strongly modulated by the state of large-scale convection. Compared to suppressed conditions, the MJO changes the radiative part of the net energy balance by about -120 W/m². Changes in sensible and latent heat flux increase the net cooling by

another 45 W/m² for a total range between suppressed and MJO conditions of about 165 W/m². The changes in radiative heat balance are strongly correlated (on the order of 0.8) with cloud fraction.

Acknowledgments.

The authors wish to thank the officers and crew of R/V *Revelle* for outstanding support for the field work. We also thank Jim Moum, Ren-Chieh Lien, and Rob Pinkel for heavy lifting associated with being Chief Scientist. This work was supported by the Office of Naval Research and the NOAA Climate Program Office.

References

Cronin, M. F., N. Bond, C. W. Fairall, and R. A. Weller, 2006: Surface cloud forcing in the Eastern Tropical Pacific. *J. Clim.*, **19**, 392-409.

Fairall, C. W., J. E. Hare, T. Uttal, D. Hazen, Meghan Cronin, Nicholas A. Bond, and Dana Veron, 2008: A seven-cruise sample of clouds, radiation, and surface forcing in the Equatorial Eastern Pacific. *J. Clim.*, **21**, 655-673.

Pincus, R., M.B. Baker, and C.S. Bretherton, 1997: What controls stratocumulus radiative properties? Lagrangian observations of cloud evolution. *J. Atmos. Sci.*, **54**, 2215–2236.

Ramanathan, V., B. Subasilar, G.J. Zhang, W. Conant, R.D. Cess, J.T. Kiehl, H. Grassl, and L. Shi, 1995: Warm pool heat budget and shortwave cloud forcing: A missing physics? *Science*, **267**, 499–503.

Webster, P. J., C. W. Fairall, P. W. Hacker, R. Lukas, E. F. Bradley, and S. Godfrey, 2002: The Joint Air-Sea Monsoon Interaction Experiment (JASMINE) Pilot study. *Bull. Am. Met. Soc.*, **83**, 1603-1630.

Experiment	Solar	LW	SENSIBLE	LATENT	RAIN	NET
TOGA COARE PILOT	197	-43	-12	-116	-3	22
TC-1	222	-58	-7	-89	-1	65
TC-2	166	-46	-11	-117	-4	-12
TC-3	190	-51	-10	-112	-3	13
TC Undisturbed	247	-57	-5	-84	-1	99
TC Disturbed	158	-43	-11	-150	-5	-51
JASMINE-2	205	-43	-9	-125	-2	27
JASMINE STAR 1 (UND)	260	-49	-5	-115	0	92
JASMINE STAR 2 (DIS)	128	-31	-17	-162	-7	-89
TC all	198	-49	-8	-105	-3	34
JASMINE all	217	-42	-6	-109	-2	62
EPIC (East Pacific UND)	224	-33	-8	-80	0	102
EPIC (East Pacific ITCZ)	163	-42	-19	-128	-7	-33
DYNAMO leg2	216	-42	-10	-126	-2	30
DYNAMO leg3	214	-41	-11	-122	-2	38
DYNAMO Undisturbed	256	-59	-6	-102	0	90
DYNAMO disturbed	206	-50	-9	-95	-2	50
DYNAMO mjo	140	-45	-18	-135	-6	-62

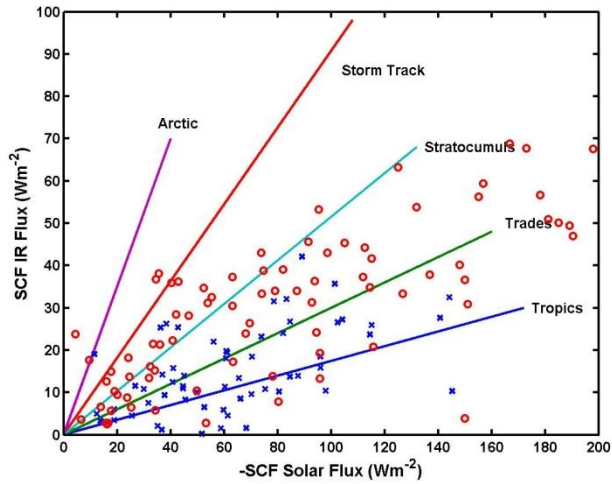


Figure 1. Cloud forcing phase diagram showing the balance of solar and IR SCF in different climate zones. An ensemble of individual days in a particular region tend to lie along a line where values near zero from small cloud fraction and values near the maximum are for cloud fraction near 1.0. The data shown here are from the EPIC field programs within 10 deg. of the equator in the E. Pacific. Symbols are: Circle — fall; x — spring.



Figure 2. R/V Roger Revelle on station in the Indian Ocean during DYNAMO..

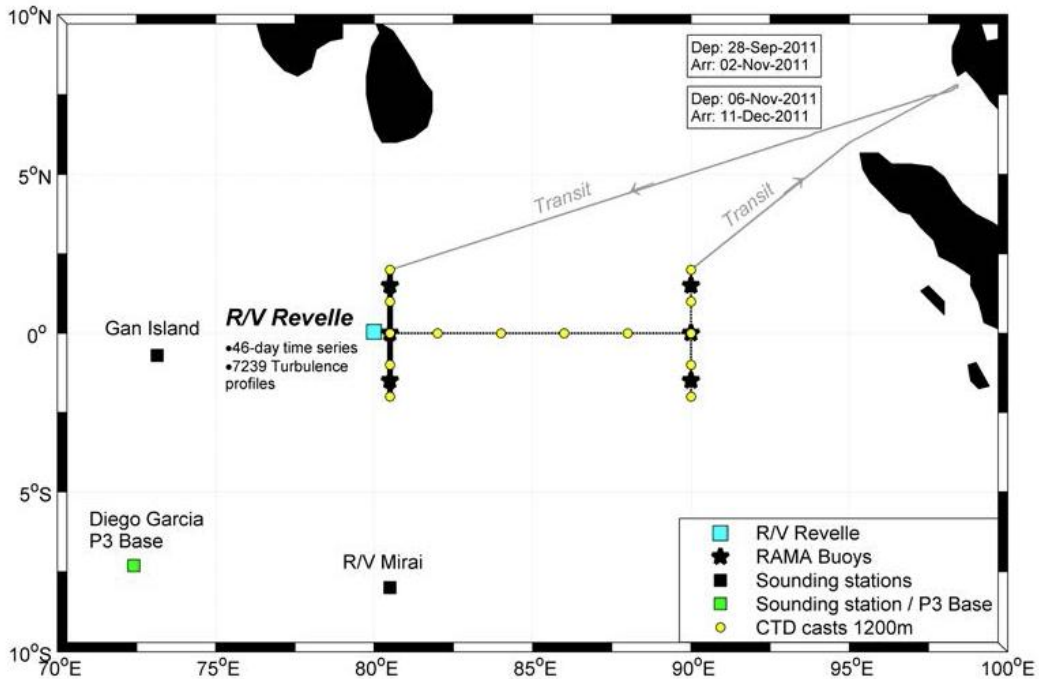
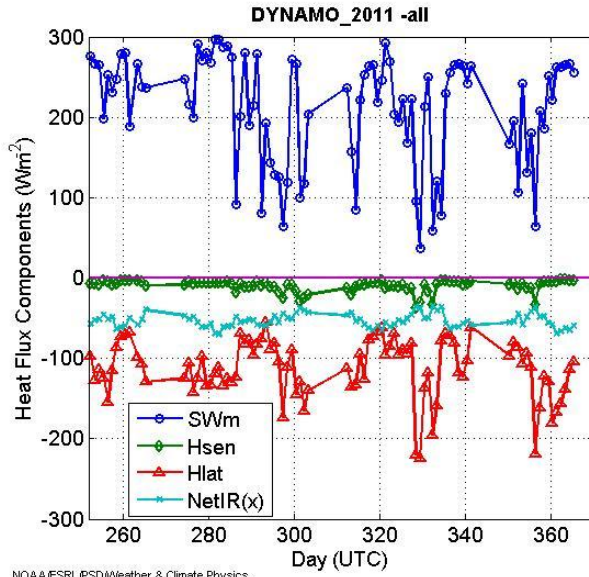


Figure 3. DYNAMO region and cruise tracks for legs 2 and 3.



NOAA/ESRL/PSD/Weather & Climate Physics

Figure 4. Time series of daily-averaged heat flux components from R/V Revelle during DYNAMO.

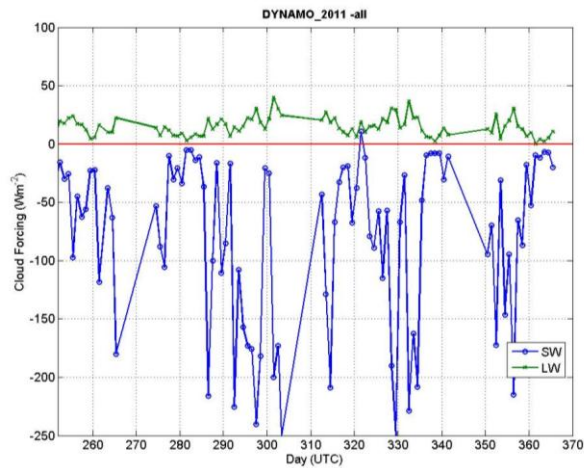


Figure 5. Time series of daily-averaged SFC during DYNAMO: blue line, solar; green line, IR.

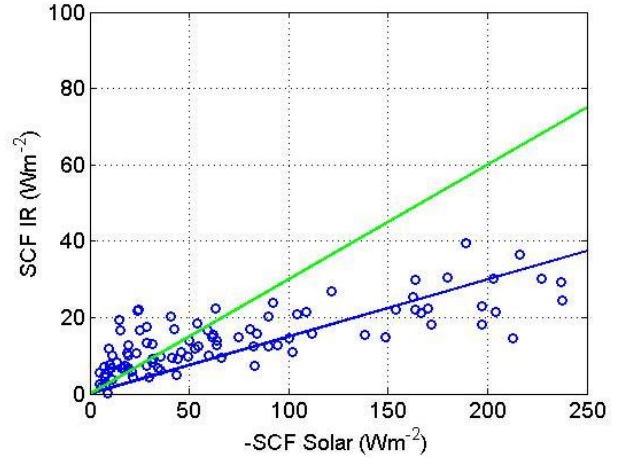


Figure 6. Cloud forcing phase diagram for daily-averaged DYNAMO observations.

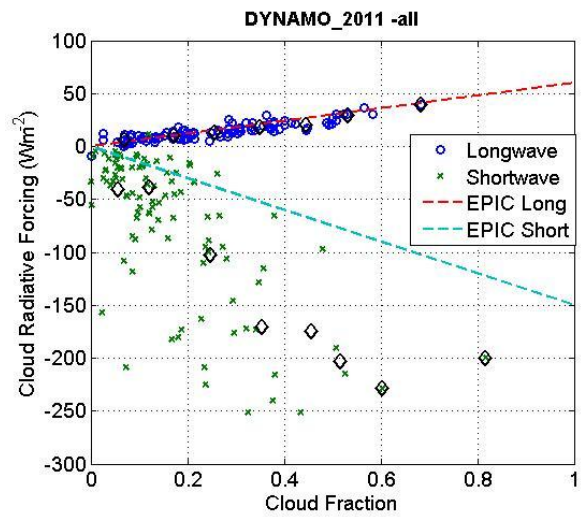


Figure 7. Solar and IR SFC as a function of cloud fraction. Individual daily values: circles (IR) and x's (Solar); Cloud-fraction bin averages are diamonds. The dashed lines are the fits to the EPIC data.

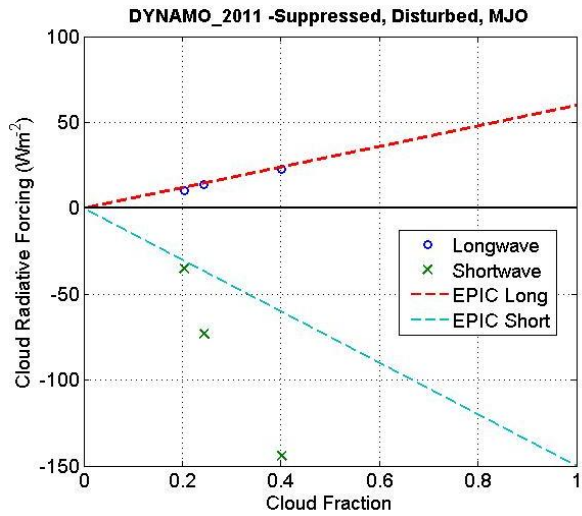


Figure 8. As in Fig. 7, but mean values computed for suppressed, disturbed, and MJO conditions.

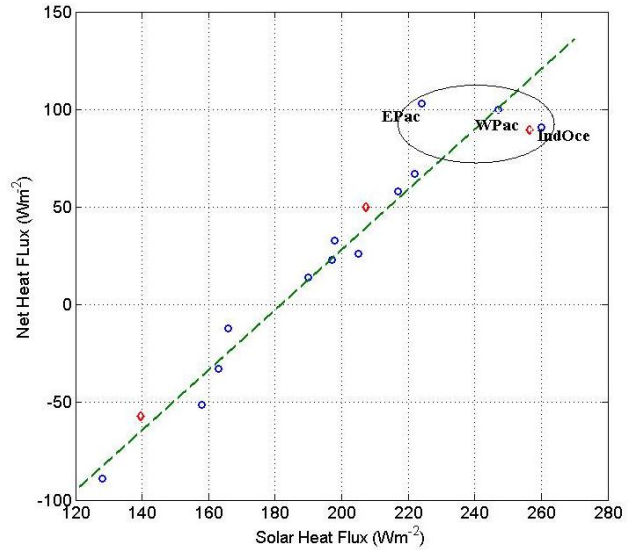


Figure. 10 Correlation of net surface energy budget with solar flux from various tropical field programs (see Table 1). DYNAMO values are in red.

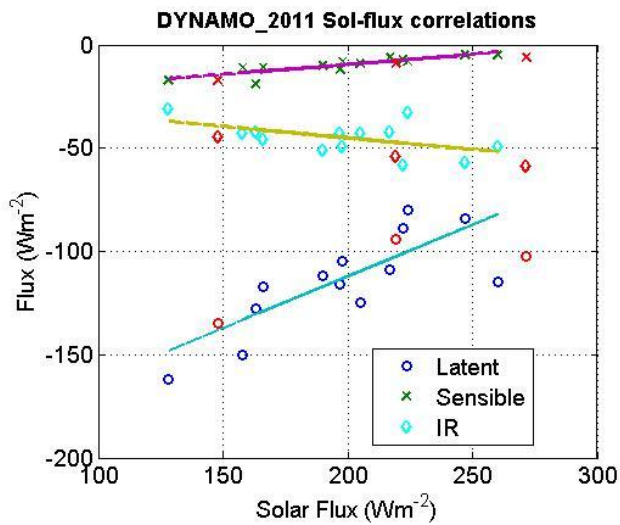


Figure 9. Correlation of flux components with mean solar flux values from Table 1. DYNAMO values are in red.